Effect of quasi-two-dimensional confinement on the dynamics of a plume thermal

Maxime Rey, with Michael MacRaild, Supervised by Julien Landel

4th year MPhys Project, 2 days/week for a semester (∼28days),
School of Physics and Astronomy,
The University of Manchester, Oxford Rd, Manchester, M13 9PY, UK

Abstract

A quasi two-dimensional thermal is studied here. A thermal is a suddenly released buoyant cloud. Quasi-two-dimensional means that its movement is restricted on two axes by using a cuboid tank with one of the three characteristic lengths far smaller than the two others. It was studied both theoretically and experimentally. The evolution in a laminar flow at $R_e < 500$ and in a turbulent flow $R_e > 2000$ were considered and their growth was expected to respectively follow laws in t^2 and as $t^{\frac{2}{3}}$. As the laminar flow has a behavior similar to the three-dimensional case, the turbulent flow was further examined. Its expansion proved drastically different than the non-restricted motion in which a mushroom shape is created. Indeed, in the quasi-two-dimensional case, the thermal splits into two main branches which in turn split into two other branches. Then, this pattern reiterates itself while slowing down. The theoretical model describing the height and the speed of these thermals is thought to be quite accurate as most errors were induced by the way the experiments were conducted. By comparing the expected evolution of the height and of the speed of the center of mass of the thermal, it was computed that the relative error was only of 10%. These models, respectively in $t^{\frac{2}{3}}$ and $t^{\frac{-1}{3}}$, corresponded roughly to the experimental results. Nonetheless, further analysis should be undertaken as it is possible to improve the precision on the release of the thermal, the experiments and the code used to analyse them.

Contents

Part I
Introduction

1 Physics of thermals

Definition of a thermal The two main parameters influencing fluids moving through one another are momentum and buoyancy. If a phenomenon is purely momentum driven, it will be denoted as a jet and if it is buoyancy driven, it will be called a plume. However, there can be several variations to these. For example, fountains are a combination of buoyancy and momentum. It may also vary depending on whether they are continuously supplied or not. Here, the phenomena studied are thermals, also called thermal plumes as they are a specific type of plume. A plume is continuously supplied whereas a thermal consists of a suddenly released buoyant cloud. They are often made of the same fluid as the ambient and the buoyancy force will be generated from a difference in temperature, hence the name thermal.

Origin of the study For the last decades and since the second World War with the entrainment assumption made by G. Taylor, the study of plumes has been increasingly considered. This assumption states that for a turbulent flow, the created eddies will entrain the surrounding fluid with a velocity proportional to a characteristic speed of the thermal. Taylor made this assumption by studying hot gases rising in air as plumes are phenomena that can be found in many places, as much underwater as in the air.

Importance of thermals Many plumes can be found in the actual world such as the steam from industries, oil burning or vent orifices in the ocean and they have huge consequences on the atmosphere of the earth. For example, the gases released by many industries strongly influence the air pollution. Their evolution can be studied through plumes or thermals to optimize their release and avoid their propagation in urban areas.

Thermals are crucial as they govern the evolution of mushroom clouds coming from explosions, nuclear ones for example, on earth or even on the sun. This can be useful in astrophysics but also in topical issues such as the environment or global warming which are causes for heated debates around the world. Thermals can be analyzed in some major cities called Urban Heat Islands (UHI) as they differ sharply from their surrounding in temperature [22]. For example, London is generally between 3°C and 9°C higher than its neighboring counties as Chandler (1967)[2] and Davies (2007)[4] studied. The air rising from these cities, often heavily polluted, is a thermal.

Here, the study focused on the influence of the confinement on thermals. An example of this would be an explosion confined between two walls. The aim of this project was to study this parameter more precisely.

2 Literature Review

As a consequence to the entrainment assumption conceptualized by Taylor, plumes and jets became more studied. The interest mainly rose from the paper written by Morton, Taylor & Turner (1955)[15] which derived the 3D governing equations for jet and plumes from the conservation of momentum, volume and buoyancy. They found that the volume was evolving in $t^{\frac{3}{2}}$ and the vertical velocity in $t^{-\frac{1}{2}}$. In this paper, they also developed a way to compute the constant of proportionality α from the entrainment assumption for continuous and instant sources and applied it to the atmosphere. Rouse, Yih & Humphreys (1952)[17] and Lee & Emmons (1961)[12] later applied it for thermals from heat sources and computed out values of 0.156 and 0.16 as summarized by Yuan & Cox (1995)[29].

Furthermore, in the governing equations derived by Morton, Taylor & Turner (1955)[15], it is computed that the thermal should expand proportionally with height. Scorer (1957)[20] verified that it was true through experiments in which he was rotating a copper cup containing the thermal at the water level to release it. He attested to the veracity of this and compared his results to two measurements taken in nature from Malkus & Scorer (1955)[14] and from Ludlam & Saunders (1956)[10]. Both measurements agreed with his expectations within a reasonable error margin. Later, Sanchez (1989)[19] also confirmed this conclusion through more precise laboratory experiments.

In his experiments, Scorer (1957)[20] also supposed that the ratio between the expansion and the height of the thermal was independent of the Reynolds number. Griffiths (1985)[7] did an experiment using heated oil released in a large tank of the same oil to try to attest this hypothesis. It confirmed it and Turner (1963)[24] broadened the result from a neutral surrounding to a case with an increasing buoyancy. Later on, Turner (1964)[25] also developed the equations for the velocity and the density variation governing an expanding thermal.

Also, as many results are based on an argument of self-similarity, Turner (1969)[26] studied this assertion comparing it to experiments from the ones of Richards (1963)[18] and Scorer (1957 & 1958)[20, 21] and confirmed

that it seemed reasonable. Griffiths (1985)[7] confirmed the self-similarity solution again for the viscous case.

Recently, Sanchez (1989) [19] partially solved a consequent problem concerning the creation of a thermal in a laboratory. The problem was that most thermals created in laboratory were released with momentum. He reduced this induced momentum by injecting the thermal in oil with a pipette. The experiments became more precise and he found that the entrainment constant for thermals was smaller than previous expectations.

Finally, as Turner (1969)[26] detailed, for this kind of turbulent flows, if the Reynolds number is large enough, it does not explicitly influence the overall evolution of the thermal and the lab results can then be applied to larger scales. Thus, the laboratory thermals can be used to study clouds formations or volcanoes as it was done for the Bezymianny volcanic eruption in 1956 by Gorshkov (1959)[6], one of the biggest natural thermals on earth. Noh (1992)[16] also used this to study the motion of the fluid in leads in polar oceans. Again, as the experiments can hardly be done where the phenomenon occurs, he did the experiments in a lab in a complex apparatus which he could extend to the real life case.

3 Objectives

Since the derivation of the motion equations from Morton, Taylor & Turner (1955)[15], the topic has not evolved much except concerning the precision of the various constants considered. Most works from these past decades only consisted in trying to either confirm or deny the theory proposed. Many experiments were done for this purpose and even if the outlines are very useful, these results are limited to the three-dimensional case with infinite boundaries. For occurrences such as vent orifices in the ocean where the thermal is restrained by walls, the equations have to be modified. Confined thermals can be typically found in human constructions such as gases created in power-plants or clouds from explosions in restricted spaces such as kitchens or buildings. They are also found in nature with, for example, volcanoes. When an explosive eruption occurs in a volcano, all the magma contained in the magma chamber (where the pressure builds up) is released and its evolution is confined by the conduit of the volcano. Consequently, this should be considered as a confined thermal to be properly studied and not as a thermal with infinite boundaries, but the number of people who studied this theory is not substantial. Some studies on the effect of quasi-two-dimensional restriction have been done as for example by Landel (2011)[9] who studied its impact on the structure of jets. As theoretical studies have never been done for quasi-2D thermals, it led this research in the direction of the said confinement. The aim of this research was to have a precise idea of the occurring phenomenon and the equations describing it.

4 Outline

The key point of this study is that it was supposed that the governing equation for the three-dimensional case of the thermal would not be true anymore. To address this supposition, a setup detailed in part II was used to try to create thermals. Also, in the same section are presented the qualitative and quantitative experiments that were conducted. Following these, a theory was built up as explained in part III to study the behavior of thermals in a quasi-2D environment. Finally, the results were precisely analyzed and discussed in part IV by using a code to output different parameters from the experiments and compare them to the theoretical model. To conclude, improvements that could be included in the apparatus or the experiments were presented.

Part II
Experimental setup

1 Presentation of the apparatus

To create a quasi-two-dimensional (quasi-2D) thermal, one of the three characteristic length describing the cuboid tank was made negligible compared to the other two. This way, the movement of the fluid would mainly be restricted on two axes. Thus, the core of the experiments was a tank of 1 m $\times$ 1 m $\times$ 0.01 m comprised of two *Perspex*® sheets 1cm apart and hermetically bound together. A pipe had to be connected to the bottom of the tank and to a bucket filled with clear water to fill the tank. The clear water was the ambient fluid for the experiment and the thermal was released from the top of the tank as represented in figure 1a. White pieces of paper were taped behind the tank such that the experiment inside it could be isolated from the background as shown in figure 1b. To record the videos, an *iPod*® was used with a resolution of 1080 pixels $\times$ 1920 pixels and a frame-rate of 29.9700 frames per second.

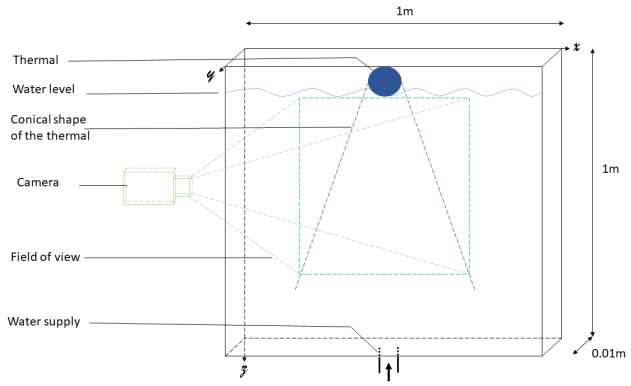

(a) Schema of the principle of the apparatus

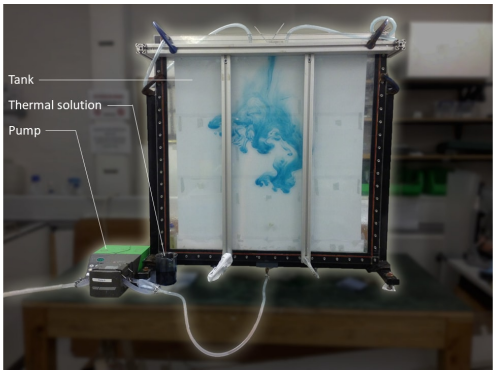

(b) Picture of the real apparatus

Figure 1: Schema and corresponding picture of the apparatus

2 Experimental procedure

2.1 Preparation

The medium used for the experiments was clear cold tap water. Since the thermal and its surrounding should have only one parameter changing, the thermal was also made of water. Dye was used in order to distinguish it from the medium and salt was added in the thermal to have a difference in density and therefore a buoyancy force.

To have proper sets of experiments (i.e. with the same thermal density), a volume V_l of thermal was produced in a beaker. The initial density of the thermal was given by equation (1). In this equation, m_s is the mass of salt added and V_l is the total volume of the solution. By taking $m_s = 5$ g and $V_l = 500$ cm^3, the initial density of the thermal was $\rho_{t,0} = 1.01$ g.cm^{-3}.

$$\rho_{t,0} = \left(1 + \frac{m_s}{V_l}\right). \tag{1}$$

For each experiment, the tank was filled with water through the pump. As the pump induced some motion in the injected fluid, it was necessary for the motion to settle down, so after being filled, the tank was left untouched for more than 10 minutes. Eventually, an appropriate volume of thermal was extracted from the beaker with a pipette and released with a specific method from the top of the tank.

2.2 Restriction on the production of a thermal

At first, many ideas were tried to create a satisfying thermal, but due to different limitations such as the small width of the tank or the necessity to have no momentum, they took a lot of time and were mostly unsuccessful. Some of them are presented here. Furthermore, several tests were done to study the effect of certain constrains on the release and the evolution of the thermal. It was done to get a proper idea of which parameters could be neglected or not when releasing it. An example would be the distance from the water at which the thermal was released.

2.3 Influence of salt

The influence of salt was also tested by comparing 2 thermals released side by side at the same time. The result after some time was obvious as demonstrated in figure 2. The sample without salt was not moving much and the one with salt was significantly faster. Salt was hence used in the experiments because if the thermals were not fast enough, the buoyancy would not necessarily be the main effect anymore as molecular diffusion could also occur. It was also important to have a thermal with a high enough speed as detailed in §2.1.4 of part IV.

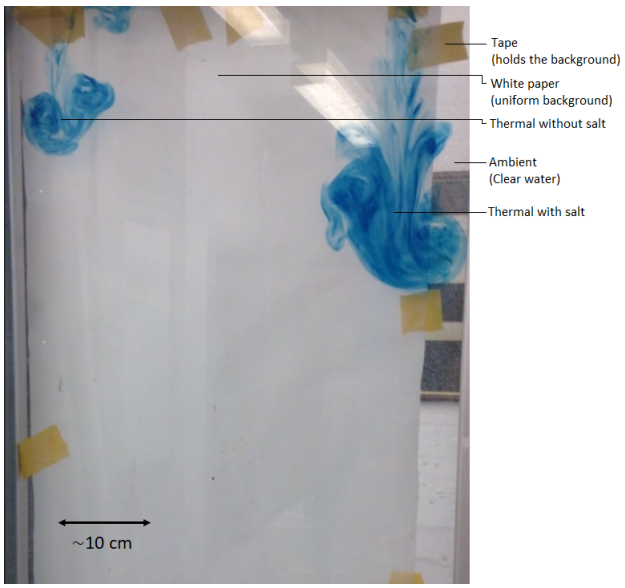

Figure 2: Difference of speed for two thermals with and without salt

2.4 Methods to create a thermal

Pipes The first satisfying way I found to produce a thermal was to submerge a part of a cylindrical pipe in the beaker and to block its extremity. This way, air was blocked in the pipe and the fluid did not leak out when removed from the solution. The amount of fluid obtained with this method could change depending on the length of the pipe submerged but it was limited to small volumes (i.e. $V < 2$ mL). If bigger pipes were used, the fluid became too heavy to be kept through pressure only. Nonetheless, when testing this method in 3D, it was confirmed that it was satisfying as a vortex ring was created, as expected from previous models.

Metal strips and oil For thermals with 2 mL $< V <$ 6 mL, I came up with a technique which used two previous methods. These two ideas were to use oil and two metal strips of dimension 100 mm $\times$ 9.70 mm $\times$ 1.95 mm coupled together as shown in figure 3b. Thanks to the metal strips, the thermal could be blocked over the oil layer. Afterwards, by releasing it, it was slowed down and thus closer to the desired rest position. This technique was the most accurate and was used for most experiments.

Triangular device To produce thermals with 5 mL $< V <$ 20 mL, I thought of using a hollow triangular device presented in figure 3a. Its shape was not important as its main purpose was to create big thermals. The principle was similar to the one in the paper of Scorer (1957)[20] who used a copper cup which he rotated. In his paper, he justifies that "the cup was turned over quickly by hand, and a negligible amount of motion was produced thereby". Some momentum was still introduced this way but it was considered negligible.

(a) Triangular object with which the thermals were released

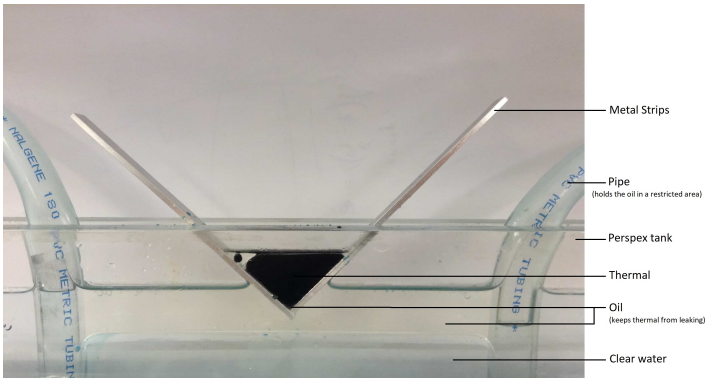

(b) Two metal strips containing a thermal in oil. It was leak-proof when on closed position

Figure 3: Final methods used to release the thermals

3 The Experiments

As not much time was available, the first experiments detailed in the section A of the appendix were qualitative and not done with a high accuracy. They were done to understand the behavior of a thermal under different conditions and to find a proper way of releasing it. In the following tables, the expansion of a quasi-2D turbulent thermal is mentioned. It describes a process in which the thermal splits into two branches which split again into smaller branches and so on.

The first experiment presented in table 1 was done in order to check if the medium was big enough to be considered quasi-infinite and if there was any back-flow occurring on the thermal. Lines of dye were produced in the tank using fluorescein: small red aggregates were dropped at the top of the tank and sunk to its bottom leaving yellowish lines on their path. The tank was immobile and the fluid in it at rest. The lines were consequently almost completely still in the tank. By then releasing the thermal and looking at the evolution of the fluorescent lines, it was possible to see to what extent it was interacting with the fluid through these lines. Furthermore, if the lines moved closer to the thermal, it meant that there was a back-flow occurring and that it was possibly interacting with the thermal (what had to be avoided).

The second experiments summarized in table 2 were the core of the projects. These are thermals produced using two metal strips immersed in oil. By rotating the strips, the thermal was released and slowed down by the oil. The volumes used for this were varying between 2 mL and 3.5 mL and the proportions of salt were either 0.04 % or 2 %.

Goal	Release method	Details	Salt percentage (mass)	Volume of thermal	Result
Determine if the tank can be considered quasi-infinite.	Two metal strips immersed in oil. Rotating them a little released the thermal.	Fluorescein was used to create lines of colored dye in the tank.	2 %	3.5 mL	The lines of dye on the furthest sides of the tank did not move.

Table 1: Experiment on the quasi-infinity (in both directions) of the tank in the y-axis.

Goal	Release method	Details	Salt percentage (mass)	Volume of thermal	Result
Analyze quantitatively a thermal to compare it with the model: set 1	Two metal strips immersed in oil. Rotating them a little released the thermal.	Number of experiments: 1	0.4 %	1 mL	The resulting thermal is too small to be analyzed.
		Number of experiments: 7	0.4 %	2 mL	The thermal falls straight for a small time and then expands as a turbulent quasi-2D thermal
Analyze quantitatively a thermal to compare it with the model: set 2	The same method as previously was used.	Number of experiments: 4	0.4 %	3 mL	Same result as previously
		Number of experiments: 4	2 %	3 mL	Same result as previously
Analyze quantitatively a thermal to compare it with the model: set 3	The same method as previously was used.	Number of experiments: 14	0.4 %	3.5 mL	Same result as previously

Table 2: Quantitative experiments of thermals using two rectangular strips and oil.

Part III
Theory

1 Key physical parameters

1.1 Assumptions

Incompressible fluid Some assumptions were necessary to deduce the movement equations and the first assumption was that the flow is incompressible. It is a common and reasonable assumption as the fluid considered was water which is almost incompressible. Since there was no strong pressure variation in the water for the experiments, this approximation did not induce errors in the calculation.

Boussinesq approximation The Boussinesq approximation had to be used to simplify the equations in the calculations. It is used in buoyancy driven flow and allows to neglect the density variation in time in a system, except when the density is multiplied by the gravitational acceleration g. When applying Newton's second law, it allowed to remove the density from the time derivative. As there was no gravity in the differential, the density of the thermal could be considered constant and removed from the time derivative. This approximation could not be applied if there was a big difference of density between the thermal and the ambient as it is the case for many phenomena, as for example volcano eruptions (the air density is 1.225 kg.m^{-3} and the density of volcano dust varies from 700 kg.m^{-3} to 3200 kg.m^{-3} [28]). For the experiments led here, this difference was small so this approximation could be applied.

Entrainment assumption The entrainment assumption states that the velocity of the fluid entrained by eddies in a turbulent thermal at any height is proportional to its characteristic velocity. The characteristic velocity chosen can be either the mean velocity at the head of the thermal or the time averaged maximum velocity [27]. The assumption $u_e = \alpha w$ was used in the calculus when applying the conservation of the volume. For a thermal plume, the value of α is typically $0.117 < \alpha < 0.199$ [29].

Quasi infinite medium Another approximation made was that the medium is quasi infinite. It means that the walls did not modify the motion of the thermal. For this purpose, I thought about doing a test to see if this was indeed true. By putting dyed lines in the tank as explained in section §3 of part II, the typical amount of fluid influenced by the evolution of the thermal could be determined. More importantly, the back-flow on the thermal could be evaluated. As expected, the thermal was only influencing a small area and there was no back-flow so this approximation was reasonable.

Diffusion process The fact that the molecular diffusion of salt and dye was negligible compared to the turbulent diffusion was checked. Indeed, the time it would have taken for the salt or the dye to spread in the tank was 8000 days for molecular diffusion whereas it was only 10 minutes for turbulent diffusion. Hence, the main cause of propagation was turbulent diffusion [3, 5, 13].

1.2 Different flow regimes: the Reynolds number

For different fluid flows, an important value that has to be considered is the Reynolds number described in equation (2). In this equation, w is the speed of the fluid, L a characteristic length, ρ the density of the fluid, μ the dynamic viscosity and $\upsilon = \frac{\mu}{\rho}$ the kinematic viscosity. The Reynolds number is the ratio between the inertial and the viscous forces, a dimensionless value which depicts the kind of flow studied. Depending on the fluid considered, the transition value between a laminar flow and a turbulent flow may change a bit but in overall, when the Reynolds number is small, the flow is laminar and when it is big, the flow is turbulent. In the experiments made for this project, the laminar-turbulent transition is typically of the order of $R_e \sim 2000$.

$$R_e = \frac{\rho w L}{\mu} = \frac{wL}{\upsilon}. \tag{2}$$

The characteristic speed of a thermal in our experiments was $w \sim 10^{-2}$ m.s^{-1} and the kinematic viscosity of water is $\upsilon \sim 10^{-6}$ m^2.s^{-1}. However, the typical length is a bit more complex. During the experiment, the thermal starts with a length $L \sim 5 \times 10^{-2}$ m or smaller but it expands with time and reaches dimensions greater than $L \sim 20 \times 10^{-2}$ m. Also, it simultaneously expands and splits into smaller thermals which in turn expand and split again into smaller branches. Considering the thermal as a whole or not will change greatly the Reynolds number. If analyzed as a single system, after some time the thermal has $R_e > 2000$. Nonetheless,

if the beginning of the experiment or if a single branch is studied, the value becomes $R_e \sim 500$ or less. There should thus be both laminar and turbulent behavior in the experiment. Hence, both flow patterns were studied.

1.3 Definition of the variables

The Cartesian coordinates (x,y,z) are used. The origin is the top left of the tank with the x-axis being perpendicular to the *Perspex*® sheets, the y-axis along them and the z-axis going downward. Here the most used axis is the z-axis as it will characterize the height of the thermal. It is important to note that the x and y axis defined here do not correspond to the x and y in the code part IV.

Here, different parameters are taken into consideration. The thermal does not have a constant defined shape through time so it is defined when it is released as a volume V. In the same way, the area which is in contact with the side of the tank is denoted as A_c and the other area on which the entrainment can occur as A_e. Finally, the width of the tank is l. If the thermal is considered cylindrical with a radius r and a length l at the beginning, considering that the experiments are in quasi-2D, its volume is $V = A_c l = \pi r^2 l$ and the entrained area $A_e = 2\pi r l$. However, as the thermal will not be a perfect cylinder at the beginning, r is taken as the "maximal radius" and variables are introduced to define its shape. Hence, with $a \leq \pi$ and $p \leq 2\pi$, equation (3) and equation (4) are obtained.

$$V = ar^2 l, \tag{3}$$

$$A_e = prl. \tag{4}$$

1.4 The initial conditions

To integrate the equations obtained later on, initial conditions are needed. They are the initial velocity, the initial radius and the initial time at which the thermal is released. In order to handle them, a virtual origin is created. The thermal is considered to be released in the experiment at a time t_1 with a radius r_1 and a velocity w_1. The diameter of the thermal is expected to grow linearly. It thus seems reasonable to say that at $t \to 0$ the radius $r \to 0$. Most papers even assume that $r = 0$ at $t = 0$. However, the consideration of the speed at $t = 0$ is often omitted in papers as the expected value induces a problem. In the calculations, an integrated quantity is $\frac{d\left(r^2(t)w(t)\right)}{dt}$. Then, the initial condition $r^2(t=0)w(t=0)$ is needed. Since it was considered that $r(t=0) = 0$, if $w(t=0) = w_0$ with $w_0 \in \mathbb{R}$, $r^2(t=0)w(t=0) = 0$. That is the assumption usually made for this calculation. Nonetheless, by doing this approximation, the variation of the speed obtained with the calculations is $w(t) \propto t^{-\frac{1}{n}}$, $n = 3$ for quasi-2D and $n = 2$ for 3D. There is consequently a singularity at $t = 0$. As $t \to 0^+$ the speed $t \to \infty \notin \mathbb{R}$. As a matter of fact, if $w_0 \in \overline{\mathbb{R}}$, it cannot be stated mathematically that $r^2(t=0)w(t=0) = 0$ as it was surreptitiously supposed in some past papers. However, another assumption can be made. As stated earlier, at the beginning of the experiment, the thermal can be considered laminar. As its radius is small, the Reynolds number corresponds to a laminar flow. Subsequently, the thermal firstly evolves with a laminar motion and then only with a turbulent motion. Since for the laminar case $w(t)' = g't + w_0$, the approximation that $r^2(t=0)w(t=0) = 0$ can be used.

2 Governing equations

2.1 Buoyancy parameter

In these experiments, a reduced gravity is defined. It is the equivalent of the gravity that the thermal experiments through its evolution: $g' = \left(\frac{\rho_t - \rho_a}{\rho_a}\right) g$. The variable ρ_t is the density of the thermal and ρ_a the density of the ambient fluid. The latter is considered to be constant as the amount of water in the tank is far larger than the density of the thermal (10 L $\gg$ 5 mL). Furthermore, the tank is considered quasi-infinite, so the quantity of water can also be considered quasi-infinite for these experiments.

After a certain amount of time, as some of the ambient fluid has been entrained and mixed with the thermal, it has a different volume and a changed reduced gravity: $g''.V'$. This entrainment leads to a change of V to $V' = xV$ and a change of density: $\rho'_t = \frac{\rho_t + (x-1)\rho_a}{x}$. Then g' becomes $g'' = \left(\frac{\rho'_t - \rho_a}{\rho_a}\right) = \left(\frac{\left(\frac{\rho_t + (x-1)\rho_a}{x}\right) - \rho_a}{\rho_a}\right) g = \frac{g'}{x}$. As a result, equation (5) is obtained, B being a constant called the buoyancy parameter.

$$g''.V' = g'V = B. \tag{5}$$

2.2 Volume conservation

The second equation comes from the fact that the differential volume change of the thermal corresponds to the expansion over time of the area through which the fluid is entrained. This area is A_e as defined earlier, and by denoting u_e the entrainment rate, the equation is given by $\frac{dV}{dt} = A_e u_e$.

Substituting the volume $V = ar^2 l$, the entrained area $A_e = prl$ and using the entrainment assumption $u_e = \alpha w$, the equation develops into $al\frac{dr^2}{dt} = plr\alpha w$. As a and l are constants in time, they can be removed from the time derivative. Also, $\frac{dr^2}{dt} = 2r\frac{dr}{dt}$ so by substituting and simplifying by $2r$, the equation can be reduced to equation (6).

$$\frac{dr(t)}{dt} = \frac{p\alpha}{2a}w(t). \tag{6}$$

2.3 Newton's second law

From Newton's second law, the derivative of the momentum is equal to the sum of the forces. Here, the momentum is $\rho V w$ and the forces acting on it are the buoyancy and the gravity. However, with the reduced gravity, the thermal can be considered as a falling object with the gravitational force given by the reduced gravity. Subsequently, the forces acting on the body can be reduced as $\rho_t V g' = \rho_t B$. The frictional forces on the two areas A_c have been ignored here as explained earlier, so Newton's second law develops into $\frac{d(\rho_t V w(t))}{dt} = \rho_t B$.

Since the Boussinesq approximation is made, ρ_t can be removed from the time derivative (as it is not multiplied by g) and be simplified with the density on the right-hand side of the equation.

Also, since $V = ar^2 l$ (a and l constants), by dividing both sides by al, the equation can be rewritten as $\frac{d\left(r^2(t)w(t)\right)}{dt} = \frac{B}{al}$

Finally, by integrating, using the initial conditions detailed in section §1.4 and dividing by $r^2(t)$, the equation is simplified to equation (7)

$$w(t) = \frac{B}{al}\frac{1}{r^2(t)}t. \tag{7}$$

2.4 Consideration of friction

2.4.1 Equation of friction

In the model, friction should also be considered. Since the experiments are restrained to a quasi-2D case, there is going to be friction at the walls of the tank using the Darcy-Weisbach equation $\frac{\Delta p}{L} = f_D \frac{\rho}{2}\frac{\langle w\rangle^2}{D}$ [1] with w as the mean-flow velocity, ρ the density, p the pressure and L a typical length. By adapting the hydraulic diameter which describes the constraints from the tank on the fluid and the Darcy friction factor, I could compute a precise formula for the frictional force. The hydraulic diameter is $D = 4\left(\frac{prl}{2pr}\right) = 2l$ and for a Reynolds number $Re \sim 2000$, the friction factor is $f \sim \frac{0.0791}{Re^4}$. By then considering that the force induced by friction was $F_f = p.A_c$, I could derive equation (8).

$$F_f = \left(4\frac{0.0791}{R_e^{0.25}}\right)\left(\frac{\rho L}{2}\right)\left(\frac{\langle v\rangle^2}{2l}\right)2ar^2 = 0.0791\left(\frac{L}{l}\right)\left(\frac{2a}{R_e^{0.25}}\right)\rho\langle v\rangle^2 r^2. \tag{8}$$

However, by adding this in Newton's second equation, the system became unsolvable. Hence, a study comparing the order of magnitude of the different forces applied in Newton's second equation was done. $\frac{d(\rho V w(t))}{dt} = \rho V g' - F_f$ with F_f still being the frictional force.

2.4.2 Comparison of the order of magnitude

The buoyancy force The buoyancy term is $\rho_t V g' = \rho_t V\left(\frac{\rho_t - \rho_a}{\rho_a}\right)g$ as explained in more detail in section §2.3. Substituting the density with equation (1) (here $\rho_a = \rho_l$), the buoyancy force is approximately given by equation (9). This is an approximation since the density considered is the one at the beginning, but it didn't vary much throughout the experiment.

$$\rho_{t,0} V g' = \left(1 + \frac{m_s}{V_l}\right) V \left(\frac{\left(1 + \frac{m_s}{V_l}\right) - \rho_l}{\rho_l}\right) g. \tag{9}$$

By taking the values $m_s = 1$ g, $V_l = 500$ cm^3, $\rho_l = 1$ g.cm^3 and $V = 1$ cm^3 the buoyancy force is$\rho_t V g' = 3.96 \times 10^{-4}$ N.

A lower concentration of salt (i.e. a lower density of thermal) and a low volume were used in this calculation so that the result is lower than the ones for the experiments. This way, if it is found that $F_f \ll \rho_t V g'$ it means that the frictional term can be neglected with a comfortable margin.

The frictional force From Khan (2015) [8], the frictional force and the shear stress are correlated by$\tau = f\left(\frac{\rho\langle v\rangle^2}{2}\right)$. As the shear stress has the unit of a force per unit area, the frictional force is given by multiplying the shear stress by the area of contact between the thermal and the tank $2A_c = 2\pi r^2$ defined earlier. Considering that the volume is $V = \pi r^2 l$, the relation $r^2 = \frac{V}{\pi l}$ is obtained and then equation (10).

$$F_f = f\rho_{t,0}\langle v\rangle^2 \frac{V}{l}. \tag{10}$$

The speed of the thermal is taken as an upper boundary. Then, if the inequality $F_f \ll \rho_t V g'$ is still verified, it means that it is true for slower speeds. As it took more than a minute for the thermal to reach the bottom of the tank (1m), the upper value $\langle v\rangle \sim \frac{1}{60}$ m.s^{-1} was taken. With $f \sim 0.007$, (from Landel (2011) [9] who used the same apparatus), a volume of 5 mL = 5 cm^3 and the same values as in the last paragraph for the other variables, the frictional force obtained is $F_f = 9.82 \times 10^{-9}$ N.

2.4.3 Conclusion on the frictional force

Even though the radius of the thermal will change over time, it is possible to not take it into account as both the friction and the buoyancy are in r^2: their ratio is going to be independent in r as they will cancel each other out. Finally, having 9.82×10^{-9} N $\ll 3.96 \times 10^{-4}$ N, the conclusion that $F_f \ll \rho_t V g'$ can be made. The frictional terms in the equations can thus be neglected.

3 Solutions for the two regimes

3.1 Turbulent theory in quasi-2D

By substituting equation (7) in equation (6), the equation $\int_0^t r^2(t)\frac{dr(t)}{dt}.dt = \int_0^t \frac{\alpha p B}{2a^2 l}t.dt$ is obtained. Integrating and taking the cubed root, it becomes equation (11) with $r(t=0) = 0$.

The equation (11) can then be substituted in equation (7) to develop into equation (13).

Finally, as $w(t) = \frac{dz(t)}{dt}$, equation (12) can be computed easily.

$$r(t) = \left(\frac{3p\alpha B}{4a^2 l}\right)^{\frac{1}{3}} t^{\frac{2}{3}}, \tag{11}$$

$$z(t) = \left(\frac{4}{3p\alpha}\right)^{\frac{2}{3}}\left(\frac{aB}{l}\right)^{\frac{1}{3}}\frac{3}{2}t^{\frac{2}{3}}, \tag{12}$$

$$w(t) = \left(\frac{4}{3p\alpha}\right)^{\frac{2}{3}}\left(\frac{aB}{l}\right)^{\frac{1}{3}} t^{-\frac{1}{3}}. \tag{13}$$

3.2 Laminar theory in quasi-2D

Entrainment occurs through eddies which are turbulent phenomena. There are no eddies and no entrainment for the laminar case, therefore $u_e = 0$.

Subsequently, the volume conservation given by equation (6) becomes $\frac{dV}{dt} = A_e u_e = 0$. Thus $V = constant$ and equation (14) is obtained.

Newton's second law, equation (7) can be written as $\frac{d(\rho V w(t))}{dt} = \rho V g'$. With no volume change and with the Boussinesq approximation, the equation reduces as $\rho_t V\frac{dw(t)}{dt} = \rho_t V g'$ and then equation (16) with w_0 constant set as $w_0 = 0$.

Also, as $w(t) = \frac{dz(t)}{dt}$, by integrating, the equation becomes equation (15), with z_0 constant set as $z_0 = 0$.

$$r(t) = Constant, \tag{14}$$

$$z(t) = \frac{1}{2}g't^2, \tag{15}$$

$$w(t) = g't. \tag{16}$$

Part IV
Results

1 Qualitative analysis

1.1 Intuitive idea

As in the three-dimensional case, the laminar case was fairly explicit. The thermal did not entrain any fluid and kept a self-similar shape. In quasi-2D, this was also the case and the thermal fell straight down. Nevertheless, if a turbulent thermal was released in 3D, it created a vortex ring which expanded with time and fell down in the apparatus. In quasi-2D, due to restriction the thermal couldn't evolve in this way. A first intuition on the behavior of the quasi-2D thermal evolution could be seen with a simple experiment. It consisted in releasing a thermal small enough so that its environment could be considered 3D at first. While expanding, the thermal did meet the quasi-2D restriction and evolved accordingly. As expected, at first a vortex ring was created and it was growing bigger as illustrated by figure 4a. As it was growing, it became more and more restrained and could not develop in the x direction anymore, but it could still spread in the y-direction. Subsequently, the thermal did split as represented in figure 4b and each branch created another vortex ring.

1.2 Empirical description

This approach started to explain how the turbulent thermal evolved in quasi-2D. The thermal which was in quasi-2D from the start did grow to create a vortex ring, but it couldn't keep expanding due to the space restriction and thus split into two. Indeed, a revolution of this image around the center of the thermal would exhibit a vortex ring as it did with the 3D case. Afterwards, the difference with the 3D case was that each of the two branches could now behave as the initial branch did and create a secondary vortex ring. While each branch split, it also started to rotate around itself creating eddies. This is identical to the phenomenon occurring in the vortex ring which rotates around itself. The process then repeated itself. At the center of the thermal, interactions occurred between the branches of the thermal and the motion became more complex . At the same time, at the edge of the thermal, the only interactions came from the ambient. Thus, the branches behavior was not changed and straight lines were distinguishable. It produced a conical shape as pictured in figure 4c

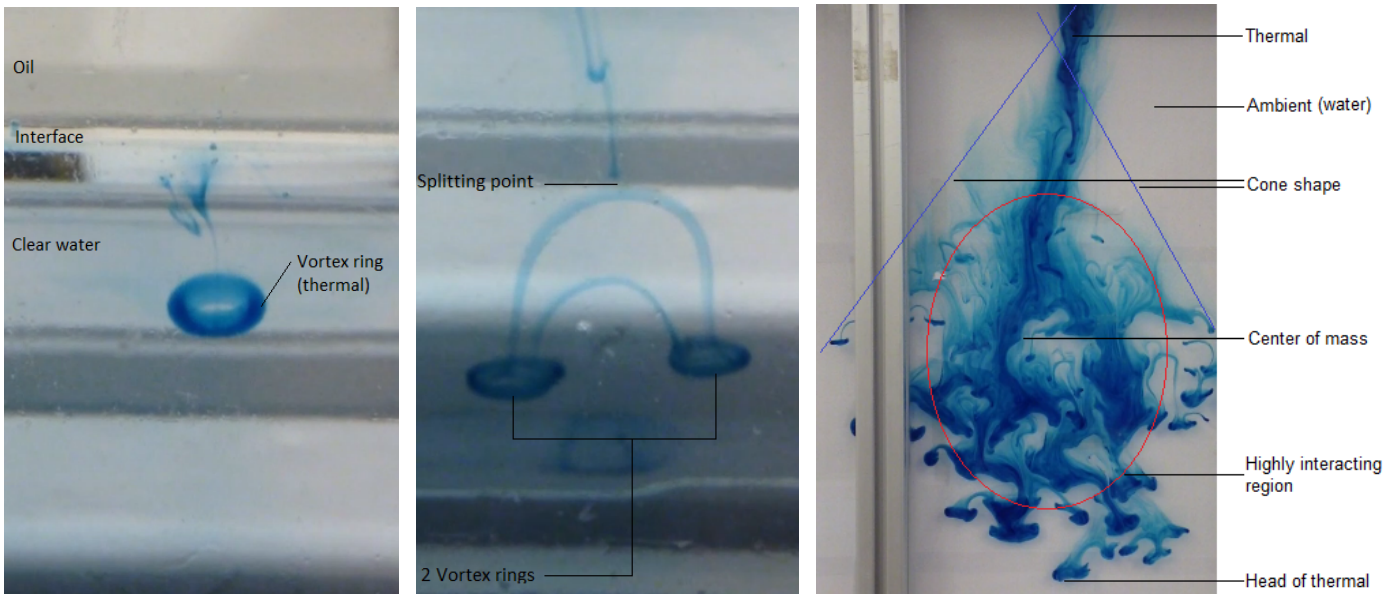

(a) Small thermal creating a vortex ring

(b) Vortex ring constrained in 2D splitting into 2 parts creating other vortex rings

(c) Typical thermal a few minutes after the release

Figure 4: Thermal evolving between 3D and quasi-2D

1.3 Phenomenological study of the volume influence

In order to study the influence of the volume of the thermal and choose which one we would study, we used the triangular device described earlier. Two sets of tests with a different amount of salt were done, each with

volumes of 5 mL, 10 mL, 15 mL and 20 mL as detailed in section §3 of part II. The samples with a higher proportion of salt had some momentum at the beginning but did split as we expected them to do. The ones without much salt had less momentum. The 4 volumes studied seemed to behave in a similar way but if the volume was increased, the shift to the turbulent thermal was occurring later. Also, if a lot of salt was added, it appeared that the thermal had more momentum when released. Since the turbulent diffusion was more defined and distinguishable with small volumes and small amounts of salt, the thermals used were created with an amount of salt of either 0.04 % or 2 % and a volume of less than 5 mL. It was also convenient as using bigger volume could have resulted in the thermals spreading off-camera.

2 Quantitative analysis

2.1 Code

2.1.1 Core principle of the code

A code was used to compute the height and the speed of the thermal from the videos and compare it to the theory. It is fully detailed in section §C of the appendix. *Matlab*® was advised for this sort of analysis so I learned it and did the code detailed afterwards. In this section the x and the y are different than before. Since matrices were considered, x was horizontal and y was vertical. Also, the origin was not placed on the tank anymore but on the top left of the recorded image.

The principle of the code was to cut the videos so that each frame could be studied individually. For each frame, the matrix of the picture was extracted, and the head of the thermal and its center of mass were computed out. It was expected to have a better match between the model and the center of mass than between the model and the head of the thermal. As the head of the thermal moved down, it may have been subject to many variations and interactions with others branches produced by the thermal. Since the center of mass is a more general variable, it depicted a better characteristic velocity.

Afterwards, by comparing two frames, the instantaneous speeds of the thermal could be calculated by dividing the distance traveled by the time between two frames. As the calculations were done for each frame, they had to be minimized: they increase the complexity of the code i.e. the computational time. Also, during the creation of the algorithm, I took into account that it may be used by other students next year as there are a lot of interesting things that were not studied here by lack of time. Thus, I added some commands not necessary for our experiments but which do not influence the complexity.

2.1.2 Delimitation of a thermal

Since a blue thermal was used on a mostly white background, I used this factor to determine the contour of the thermal. As explained earlier, the molecular diffusion (of either salt or dye) was negligible before the turbulent diffusion so the dye could be considered to be a good proxy for the thermal. The assumption was pushed further by saying that the "blueness" of the thermal was in fact a good proxy for its density. If the thermal was dark blue, it was considered denser than if it was light blue.

Also, the images are encoded in the RGB (Red, Green, Blue) system on a matrix with the values of the pixels comprised between 0 and 255 (coded on 8 bits). It means that for a colored image of 1920 pixels $\times$ 1080 pixels, the matrix has a dimension of 1920 $\times$ 1080 $\times$ 3 in pixels. These 3-color matrices added together then displayed approximately 1.6×10^7shades of visible colors that the human eye can see as in figure 5a. Their absence is seen as black (i.e. 0 for each) and their presence is seen as white (i.e. 255 for each).

I used this to distinguish the thermal from the ambient. As the goal was to highlight the blue of the picture, I took the values of the first and the second matrix $(R + G)$ and added them together as in figure 5b. All the pixels containing some red or green thus took higher values and became brighter. The blue thermal which only contained a negligible amount of red and green was displayed as really dark.

For practical reasons, a matrix where high values of pixel meant high concentration of dye was aimed for so I took the complementary value of each pixels as displayed in figure 5c. Then, a value from which the pixel could be considered blue enough to be in the thermal had to be chosen. If this value was too high, some parts of the thermals would be missed and if it was too low, other parts than the thermal would have been taken by the code as the thermal. By looking at different thermals, it was determined that the pixel belongs to the thermal if the value is more than $D = 140$. There was no blue (or any color containing blue) in the frame except the thermal and there was a program made to remove any blue in the surrounding of the thermal. However, if a smurf were to hop in front of the thermal during a video, there would be no way of getting rid of it, the video would either have to be cut in time just before the interference (and then the graphs too) or discarded.

(a) Picture of a thermal

(b) Picture of a thermal with the R and G part of the matrix added together

(c) Negative of a picture of a thermal with the R and G part of the matrix

Figure 5: Visualization of the manipulations made on the thermal throughout the code

2.1.3 Computations on the head of the thermal and of its barycenter

Height of the head of thermal (HoT) To know the position of the thermal, I did a function which was going through all the columns and then all the lines of the matrix. For each line in a said column, I only took into account the pixels that had a value higher than D. Amongst these pixels, I took the one which was the closest to the bottom of the tank by comparing the values associated to the line the pixels were on. Indeed, as said before, the lower the position in the tank is, the higher the y-value is. For each column, I thus had a "maximum pixel" which defined by its position a local HoT. Afterwards, by comparing all these pixels and taking the one with the highest value, the lowest one in the tank, the HoT was obtained. Obviously, the speed obtained from this was the speed projected on the y-axis, as only the value of the height of the HoT was taken.

Height of the Center of mass (CoM) The CoM was obtained through a similar but more complex process as the density of the thermal had to be taken into account for the x and the y coordinates. Since it is the CoM which is computed here, each pixel was considered with a different value regarding its density. This was done by using the value of the pixel in the matrix: the higher it was, the denser it was.

To get the x-coordinate of the CoM, the algorithm first went through all the columns and for each of them, added up all the values of the thermal's pixels. The total density of each column TD was thus obtained and the barycenter of this equivalent row in x was the barycenter of the matrix in x. Afterwards, a variable WD was created for the sum of the densities of each column multiplied by the x coordinate of the column. This corresponded to a weighted density. The x-coordinate was then given by the ratio of the weighted density to the total density as shown more consistently by equation (17). D is the density of a pixel, j the x coordinate of a column. $TD = \sum_{columns}(\sum_{rows} D)$ and $WD = \sum_{columns}(\sum_{rows} D) * j$.

It was symmetrically done for the y-coordinate and the output of the function was the round value of both coordinates as they have to be integers since they are a length in number of pixels.

$$Barycenter(x) = \frac{\sum_{columns}(\sum_{rows} D * j)}{\sum_{columns}\sum_{rows} D}. \tag{17}$$

Calculation of the speeds of the thermal Having the coordinates of the HoT and the CoM for each frame and the time between them, a new array of dimension (NbFrame-1) was created to store the corresponding instantaneous speed. To get them, the distance traveled between two frames was divided by the time it took.

2.1.4 Major limitation: the frame-rate and the resolution

When plotting the computed data, there was a problem: the values were either 0 or a constant. I found that it was due to the frame-rate being too high regarding the resolution. The thermal did not have the time to travel more than a pixel between two frames. It was so slow that the time it took to go from one pixel to another was lower than the time separating two frames. Two outcomes were then possible. Either it did not have the time to

go to the next pixel and the speed was 0 pixels/frame, or it had the time and traveled one pixel (sometimes two pixels when it was a bit faster). The constant obtained was therefore the length of a pixel (the length between the middle of two pixels) divided by the time between two frames.

Hence, some frames in the code had to be skipped. However, *Matlab*® does not allow to skip frames so I had to code it. To know how many loops should be skipped, the frame-rate F had to be taken into account as well as the real length of a pixel P, the minimal speed of the thermal u_{min} and the smallest number of pixels that the thermal should travel between two frames when it was at its slowest speed n. Therefore, the number of frames that had to be skipped was the integer corresponding to equation (18). Also, it was important to check that by doing so, there were still enough points to have a proper curve and study the thermal. Hence, for a video of t seconds, the number of points on the plot was be the integer part of equation (19).

$$NbSkipFrames = \frac{nPF}{u_{min}}, \tag{18}$$

$$NbPoints = \frac{FT}{NbSkipFrames}. \tag{19}$$

I chose a minimal speed of 0.1 cm.s^{-1} which gave a large margin of error. By wanting the thermal to travel at least 3 pixels when it was at its extreme lowest speed; with equation (18) and a margin, the number of frames that had to be skipped was 49. For a video of 2 minutes, using equation (19), I computed that there was 73 points, which was enough to have a proper curve. In the end, the curves were more precise for lower speeds and there were still enough points to be able to study the evolution of the thermals properly.

2.2 Results from the code for a single experiment

2.2.1 Inclusion of a virtual origin

Necessity of a virtual origin To compare the theoretical model to the experimental one, a logarithm plot was used and the equations of the type $z(t) = t^n$ became $ln(z(t)) = n.ln(t)$. Looking at the gradient of the curve then gave a precise value for the power of t considered. However, everything was shifted due to the experiments not starting with a volume V = 0 and beginning as a laminar flow even if it was turbulent afterwards. A virtual origin was thus needed and the curves plotted were of the type $z(t) - z_0 = (t - t_0)^n$ and became $ln(z(t) - z_0) = n.ln(t - t_0)$. These two parameters greatly changed the graphs as exhibited with the difference between figure 6a and figure 6b.

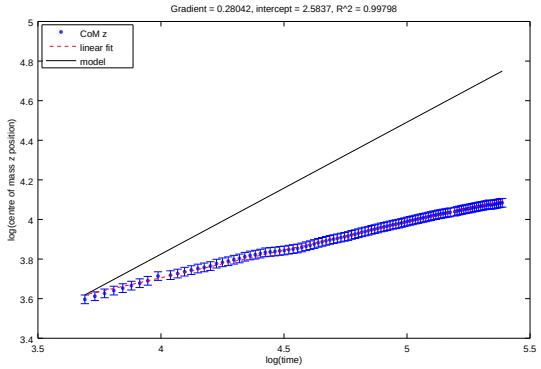

(a) Plot of the height of CoM against time without the virtual origin

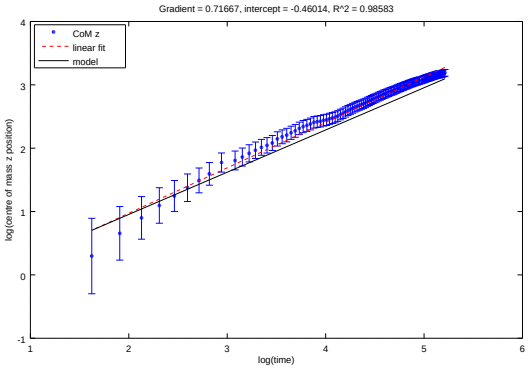

(b) Plot of the height of HoT against time with the virtual origin

Figure 6: Influence of the virtual origin on the plot of a thermal. These graphs show the barycenter of the thermal in x

Determination of the virtual origin To determine the virtual origin, the expansion of the radius of the thermal was studied and traced back to zero. Indeed, as the evolution of r(z) was linear in z, by tracing straight lines corresponding to the edge of the thermal and taking their intersection as shown by the blue lines in figure 4c, it was possible to obtain the coordinates of the virtual origin. This was done by computer. The code requested the user to take two points on each line. It computed the coordinates in x and y of the virtual origin according to the equations (20). The X and Y are arrays of dimension four which were containing the coordinates of the four points selected.

$$\begin{cases} x = \frac{Y(1)-Y(3)+m_2X(3)-m_1X(1))}{m_2-m_1}, & m1 = \frac{Y(2)-Y(1)}{X(2)-X(1)}, \\ y = \frac{m_2*Y(1)-m_1Y(3)+m_1m_2(X(3)-X(1))}{m_2-m_1}, & m2 = \frac{Y(4)-Y(3)}{X(4)-X(3)}. \end{cases} \tag{20}$$

Errors on the measures Some important parameters which I wanted to include were the uncertainties as many errors were induced. For example, the precision when the distances were measured or when the speeds were converted from pixels per frames to meters per second was limited. There was also an error which was related to how the camera took the picture. If two points separated by a distance d were taken at the top and in the middle of the tank, the corresponding distances in pixels were not the same. As the distance between the camera and the top of the tank or the distance between the camera and the middle of the tank were not the same, the corresponding measures of d were not the same. Therefore, these uncertainties were implemented in the code and on the plots.

Results for an experiment The core of the experiments were thermals of 3.5 mL released using two metal strips submerged in oil as detailed earlier. In figure 7 and figure 8, the results for a typical experiment are presented with the data points in blue, the best linear fit in red and the model in black. On top of the graph is also shown the gradient, the intersection and R^2. Since the plots are presented in a log scale, the important parameter to look at is the gradient. By considering the model given by equation (12) and equation (13), a gradient of $\frac{2}{3}$ is expected for the height of the thermal and of $-\frac{1}{3}$ for its speed.

Concerning the heights of the thermal, the error bars are quite small as the precision was rather high. The distances were of the order of 10 cm when the errors were of the order of a few pixels, which usually had a characteristic dimension of 5×10^{-2} cm. However, the errors bars for the speeds grew really high because the speed became really small with time and there was a limitation due to the resolution as explained earlier. As predicted, the gradient of the HoT was further away from the model than the gradient of the CoM.

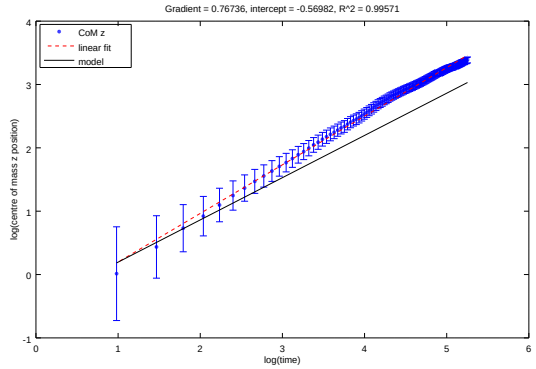

(a) Plot of the height of CoM against time for a single experiment

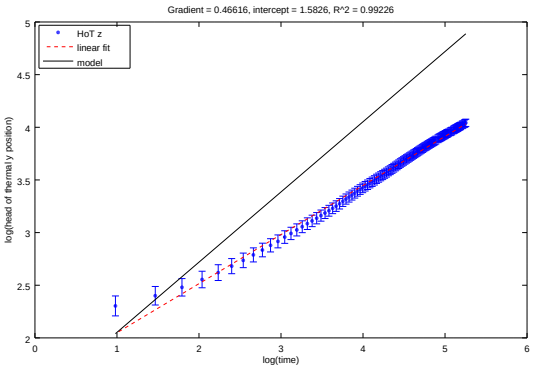

(b) Plot of the height of HoT against time for a single experiment

Figure 7: Height of the thermal against time for CoM and HoT for a single experiment

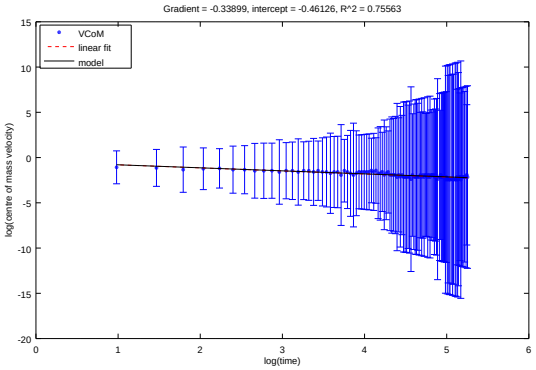

(a) Plot of the speed of CoM against time for a single experiment

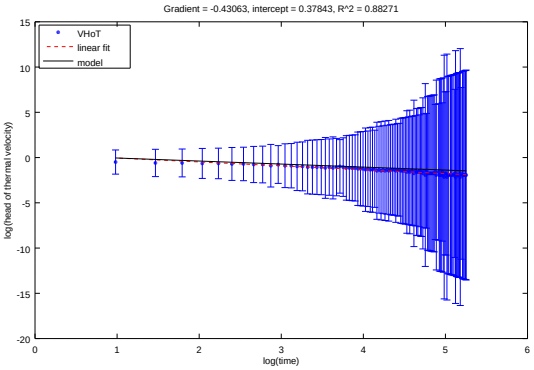

(b) Plot of the speed of HoT against time for a single experiment

Figure 8: Speed of the thermal against time for CoM and HoT for a single experiment

2.3 Presentation of a set of experiments

In this section, figure 9 shows the height and the speed of the CoM for a set of experiments. The similar plots concerning the head of the thermal are presented in the appendix section §B. In red are the best fits of the nine experiments, in blue the average of the best fits and in black the theoretical model. In these graphs, it is noteworthy that most experiments have a similar fit and that they are quite close to the model.

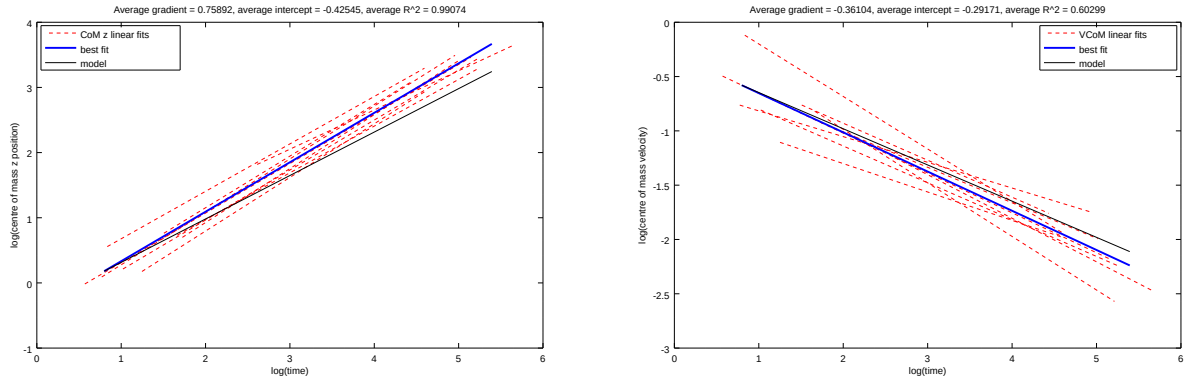

(a) Plot of the height of CoM against time for nine experiments

(b) Plot of the speed of CoM against time for nine experiments

Figure 9: Height and speed of the CoM for nine experiments

2.4 Analysis of the results

Even if the gradients of the curves seem close by looking at the absolute difference, the value considered should be the relative error on the measure given by equation (21). The relative errors from the theoretical model for the height and the speed of the CoM are respectively 12.5 % and 8 %. The fit of the data points is similar to the model so it is reasonably satisfactory but they are globally distributed over it. It means that there was a non-negligible systematic error repeated through the experiments or that a phenomenon had been omitted. Also, the distribution of the gradients means that some parameters had bigger consequences than expected. However, there are various parameters that could be introduced or improved with more time and which would give results closer to the model.

$$RelErr = \left| \frac{Value_{exp} - Value_{th}}{Value_{th}} \right| \times 100. \tag{21}$$

2.4.1 Human errors

The biggest errors were induced by the user and the method adopted to create the thermal. With the current way of producing the thermal, some momentum was generated. The thermal was poured between the metal strips and then did rest a bit before being released in the oil. In order to not induce too much flow in the water by moving the strips, they were placed on top of the oil layer. When released, the thermal had some momentum which was not totally canceled by the oil layer. Also, the virtual origin was not precise enough for these experiments. For certain thermals, the branches on the sides became really thin because the dye died out. The cone was consequently hard to determine. As the time origin was taken by looking at the data and finding the corresponding time for a said z origin, another error was introduced. Since the virtual origin changed the gradient of the plot, the result was altered.

2.4.2 Uncertainties introduced by the code

Added to these errors, the code also introduced some uncertainties as it took out values of densities for the thermal based on how blue it was. The first interference came from the shadows. As there was a metal structure to hold the tank, there were shadows generated by it. These dark shadows interfered with the center of mass and induced a shift in the intersect of the data curve with the y-axis. Besides, when the thermal was released, a little amount of it was sticking for a small time to the metal strips and was released after the first thermal. This second thermal caused a sharp bend in the evolution of the data points. The speed of the new CoM became a weighted average of the CoM of the two thermals which were at different stages of their evolution. Thus, the gradient was also different.

2.4.3 Conclusion

In the presented experiments, the evolution of the height of the thermal and of its speed were close to the theoretical model, which implies that it was indeed reasonably good and represents a satisfactory basis for future works. The relative error was still of the order of 10 %. This value is high and entails the presence of errors either in the experimentation or in the model. Many of the failures of the said experimentation could be improved through different methods, both in the apparatus itself and in the way the experiments are conducted. Implementing these may allow further studies to conclude on the accuracy of the theoretical model presented here for a turbulent thermal in quasi-2D.

Summary

In this study, we discovered that a restriction on one dimension had an interesting impact on the structure of a thermal. Indeed, in 3D, they tend to get a mushroom shape but here, with a density difference between the thermal and the ambient of 0.04 %, the initial thermal splits into two smaller branches which in turn splits into two smaller branches and so on. Furthermore, an explanation for the initial velocity of the thermal was found as it seems that the thermal evolves in a first part as a laminar flow. However, it should be confirmed that it was not due to an initial momentum given through the release, even though the method proposed by Sanchez (1989) [19] was seemingly improved. Finally, the experiments did fit reasonably the theoretical model exposed for the turbulent case of the quasi-two-dimensional thermal which were predicting an evolution of the height in $t^{\frac{2}{3}}$ and a decrease of the speed in $t^{-\frac{1}{3}}$. More experiments should now be conducted in order to enhance the accuracy of the measurements and to confirm its coherence with the model presented.

Directions for further studies

Some improvements could be introduced. Having a bigger or longer tank would allow to have either more points on the graphs (by making the thermal faster) or to study the thermal for a longer time. A camera with a better resolution would allow the same kind of improvements and could be bought inexpensively as the camera was only 2MP which is a low standard nowadays. Increasing the resolution of the camera is one of the easiest and most efficient improvement that could be done here as multiplying the resolution by ten would reduce the error by a factor ten. Also, undertaking more experiments (they are highly reproducible) would decrease the random error on the measures and it would allow the user to pick solely the experiments with a well defined cone in order to acquire a very precise virtual origin. Finally, improving the code (regarding shadows or the background) or another system of release for the thermal would reduce the systematic error. Stratified oil, a different material (to avoid a second thermal) or another design submerged in oil (for example a cylindrical device that would rotate around a fixed axis) may allow to have less momentum introduced.

As presented here, there are a lot of improvements that could still be done on this apparatus and these experiments to improve the precision of the results. The errors would be greatly reduced and a conclusion on the accuracy of the theory may be enhanced if the data points were indeed converging towards the model as expected.

Acknowledgment

This report was done for an MPhys project at the University of Manchester. I would like to give my special thanks to J. Landel for his precious advice, to M. MacRaild for his collaboration and to E. Labaume for her help.

References

[1] Brown G. 2002 The History of the Darcy-Weisbach Equation for Pipe Flow Resistance, Proc. Environ. Water Resour. Hist., vol. 38.

[2] Chandler T.J. 1965 The Climate of London, London, Hutchinson.

[3] Csanady G.T. 1973 The Fluctuation Problem in Turbulent Diffusion, Turbulent Diffusion in the Environment, pp. 222-248.

[4] Davies M. 2007 Implications of UHI Issues for Urban Planning: a London Perspective, Office of the Mayor of London.

[5] Frenkiel F.N. 1953 Turbulent Diffusion: Mean Concentration Distribution in a Flow Field of Homogeneous Turbulence, Advances in Applied Mechanics, vol. 3, pp. 61-107.

[6] Gorshkov G.S. 1959 Gigantic eruption of the volcano bezymianny, Bulletin of Volcanology, vol. 20, pp. 77-109.

[7] Griffiths R. W. 1985 Thermals in extremely viscous fluids, including the effects of temperature-dependent viscosity, J. Fluid Mech., vol. 166, pp. 115-138.

[8] Khan M.K. 2015, Fluid Mechanics and Machinery, Oxford University Press India.

[9] Landel J. R. Cauleld C. P. and Woods A. W. 2011 Meandering due to large eddies and the statistically self-similar dynamics of quasi-two-dimensional jets, J. Fluid Mech., vol. 692, pp. 347-368.

[10] Ludlam F.H, . and Saunders P.M. 1956 Shower formation in large cumulus, Tellus, vol. 8, issue 4, pp. 424-442.

[11] Lund H.M. and Dalziel S.B. 2014 Bursting water balloons, vol. 756, pp. 771-815.

[12] Lee S.L. and Emmons H.W., 1961 A Study of natural convection above a line fire, J. of Fluid Mech., vol. 11, pp. 353-368 .

[13] Majda A.J. and Kramer P.R. 1999 Simplified models for turbulent diffusion: Theory, numerical modeling, and physical phenomena, Physics Reports A. vol. 314, issues 4–5, pp. 237-574.

[14] Malkus S., and Scorer R.S., 1955 The erosion of cumulus towers, J . Me., vol. 12, pp. 43-57.

[15] Morton B.R., Taylor G., Turner J.S. 1955 Turbulent gravitational convection from maintained and instantaneous sources, Proceedings of the Royal Society of London. Series A. Math. and Phys. Sc., vol. 234, pp. 1-23.

[16] Noh Y., H., Fernando J. S., and Ching C. Y. 1992 Flows Induced by the Impingement of a Two-Dimensional Thermal on a Density Interface, J. Physical Oceanography, vol. 22, issue 10, pp. 1207-1220.

[17] Rouse H., Yih C. S. and Humphreys H.W., 1952 Gravitational Convection from a Buoyancy Source, Tellus, vol. 4, issue 3, pp. 201-210.

[18] Richards 1963 J. M. Intern. J. Air. Water Pollution, vol. 7, pp. 17-34.

[19] Sanchez O., Raymond D.J., Libersky L., Petschek A.G. 1989 The development of thermals from rest, J. Atmospheric Sc., vol. 46, No. 14, pp 2280-2291.

[20] Scorer R.S. 1957 Experiments on convection of isolated masses of buoyant fluid, J. Fluid Mech., vol. 2, issue 6, pp. 583-594.

[21] Scorer, R. S. 1958 Natural Aerodynamics, Pergamon Press, London, pp.312.

[22] Sheng-I H. 1981 The urban heat island effect: a case study of metropolitan Phoenix area, Chinese University of Hong Kong.

[23] Sreenivas K. R., Prasad A. K. 1999 Vortex-dynamics model for entrainment in jets and plumes, Phys. Fluids, vol. 12, issue 8, pp. 2101-2107.

[24] Turner J. S. 1963 Model experiments relating to thermals with increasing buoyancy, Quarterly Journal of the Royal Meteorological Society, vol. 89, issue 379, pp. 62-74.

[25] Turner J.S. 1964 The dynamics of spheroidal masses of buoyant fluid, J. Fluid Mech., vol. 19, pp. 481-490.

[26] Turner J. S. 1969 Buoyant plumes and thermal, Annu. Rev. Fluid Mech., vol.1, pp 29-44.

[27] Turner J. S. 1986 Turbulent entrainment: the development of the entrainment assumption, and its application to geophysical flows, J. Fluid Mech., vol. 173, pp. 431-471.

[28] Wilson T.M., Stewart C., Sword-Daniels V., Leonard, G., Johnston, D.M., Cole, J.W., Wardman, J., Wilson, G., Barnard, S. 2011 Volcanic ash impacts on critical infrastructure, Phys. and Chem. of the Earth. vol. 45–46, pp. 5-23.

[29] Yuan L.M., Cox G. 1995 Entrainment of line thermal plumes, AOFST Symposiums 2.

Appendix

A Tables of experiments

The following graphs detail experimentation on the thermals and the way to create them. When a variable X is used as an input for an experiment (typically for the proportion of salt), it means that it was not measured precisely but nonetheless constant for a set of experiment. Table 3 presents results obtained with pipes and table 5 was done with the triangular device, to know which volumes and proportions of salt should be considered for following experiments. Table 4 concerns experimentation on the use of oil and a pipette. The main goal was to see if big thermals could be created this way.

Goal	Release method	Details	Salt percentage (mass)	Volume of thermal	Result
Test the validity of the pipe method.	A pipe was submerged in the solution of thermal and then blocked in it by making the other extremity of the pipe air-locked.	In 3D.	X %	1 mL	A vortex ring is created.
		In quasi-2D.			The expected turbulent quasi-2D thermal is observed.
Analyze the influence of salt on the thermal.	The same method as before was used.		0 %	1 mL	The thermal with salt is more than two times faster than the other one without salt
			X %		
Analyze the influence of the height in the pipe.	The same method as before was used.	Ratio of the height in the pipe = 2.	X %	1 mL	Similar thermals.
			X %	1 mL	
Analyze the influence of the height of release.	The same method as before was used.	Released at water level.	X %	1 mL	Similar thermals.
		Released 10cm further			

Table 3: First tests with a pipe

Goal	Release method	Details	Salt percentage (mass)	Volume of thermal	Result
Create a proper thermal using oil.	A pipette was used to create a bubble in the oil. After some time the bubbles pierced the oil layer.	There was not enough dye for the experiment.	X %	~0.5 mL	A really well-defined quasi-2D turbulent thermal appears from the beginning of the release.
		Volume added to make the thermal more distinguishable.	X %	~1 mL	Similar to the previous experiment but with an added delay for the turbulent expansion.
		Number of experiments: >5 But 2 bubbles produced	X %	~1 mL	Similar to the previous experiment but a second smaller thermal is released

Table 4: Tests to create a good thermal using a pipette and oil.

Goal	Release method	Salt percentage (mass)	Volume of thermal	Result	Comparison with respect to the salt proportion
Analyze the influence of the variation of 5 mL of thermal for a low amount of salt	The triangular device was used. The thermal is poured in it and then the device is rotated at the surface of the water.	~1 %	5 mL	A 2D mushroom cloud appears first. It evolves quickly into a quasi-2D thermal.	The shape of the thermal in the second part is well defined.
			10 mL	A 2D mushroom cloud appears first. It evolves a bit later into a quasi-2D thermal.	
			15 mL	A 2D mushroom cloud appears first. It evolves slowly into a quasi-2D thermal.	
			20 mL	Similar to 15 mL.	
Analyze the influence of the variation of 5 mL of thermal for a high amount of salt	The same method as before was used	~10 %	5 mL	Same as for 1 % of salt	The mushroom shape is more persistent. The turbulent thermal develops later and does not have a well defined shape.
			10 mL	A 2D mushroom cloud is created. It keeps this shape while spreading horizontally and then evolves as a quasi-2D thermal.	
			15 mL	Similar to 10 mL but the turbulent motion develops at the bottom of the tank.	
			20 mL	Similar to 15 mL but the spread occurs on a wider area.	

Table 5: Volume and salt influence on the evolution of the thermal with the triangular device

B Presentation of a set of experiment

Here, the heights and the speeds of the HoT are presented for 9 experiments from a same set. These measures are close to the model but the errors are bigger than for the CoM. It makes sense as the CoM is an overall value and the HoT is more localized. The errors explained are thus increased for this parameter.

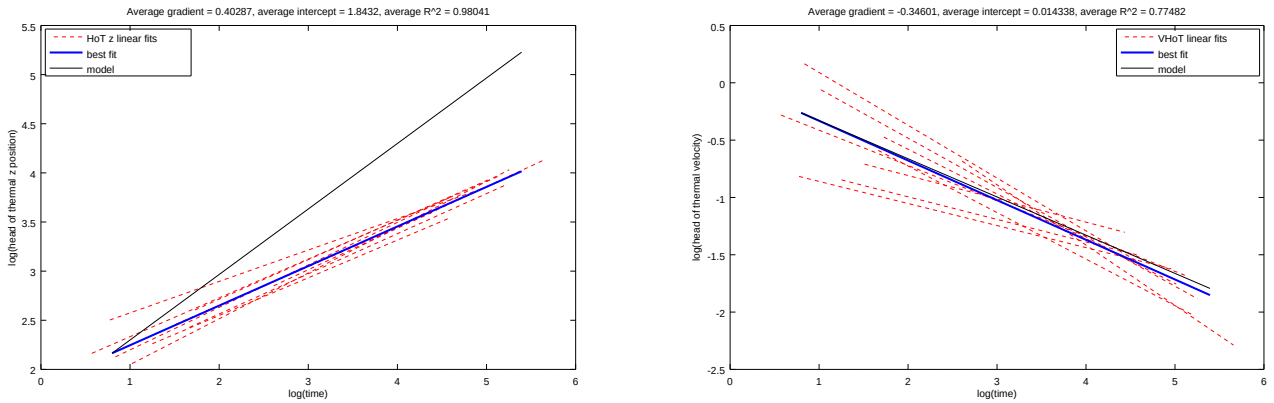

(a) Plot of the height of HoT against time for nine experiments

(b) Plot of the speed of HoT against time for nine experiments

Figure 10: Height and speed of the HoT for nine experiments

C Detailed Code

Figure 11: Core of the code

```
function [COM] = CenterofMass(img, Bounds)

I=imread(img);
IMG = (I(:,:,1)+I(:,:,2));

Bounds = floor(Bounds);
WD = 0;     %Weighted density
TD = 0;     %Total density
    for j = Bounds(3):Bounds(4)
        LD = 0;
        for i= Bounds(1):Bounds(2)
            D = 255 - double(IMG(i,j)); %take "negative" s.t. max value = more dense
            if D>140                    %if there's thermal here
                TD = TD + D;
                LD = LD + D;
            end
        end
        WD = WD + LD*j;
    end
    COMX = WD/TD;

WD = 0;
TD = 0;
    for i = Bounds(1):Bounds(2)
        LD = 0;
        for j = Bounds(3):Bounds(4)
            D = 255 - double(IMG(i,j));
            if D>140
                TD = TD + D;
                LD = LD + D;
            end
        end
        WD = WD + LD*i;
    end
    COMY = WD/TD;

    COM = [round(COMX,0) round(COMY,0)]; %coord of CoM
end
```

(a) Function CenterofMass

```
function [HoTfinal] = HeadofThermal(img, Bounds)

I=imread(img);
IMG = (I(:,:,1)+I(:,:,2));

Bounds = floor(Bounds);
HoT = [];
HoTtemp = 0; %temp = temporary
HoTfinal = 0;

    for column = Bounds(3):Bounds(4)    %go through all pixels
        for line = Bounds(1):Bounds(2)
            D = 255 - double(IMG(line,column));
            if D>140
                HoTtemp = line;

            end
        end
        HoT = [HoT HoTtemp];
    end
    for i = 1:numel(HoT)       %i = first to last element of array
        if HoT(i) > HoTfinal
            HoTfinal = HoT(i); %Height of Thermal z (one coord)
        end
    end
end
```

(b) Function HeadofThermal

Figure 12